Application of Optical Flow Method for Extrapolating Radar Echoes

Xiangqian Wei, Xinyu Chang, Yi Liu *, Jun Guo

College of Civil & Hydraulic Engineering, Huazhong University of Science & Technology, Wuhan 430000, China

*Corresponding author's e-mail: prof_liuyi@hust.edu.cn

Abstract. Short-term precipitation forecasting is one of the key challenges in meteorological predictions and plays a critical role in real-time weather disaster response and mitigation. Weather conditions are primarily obtained through radar echo information, and short-term forecasts mainly rely on the prediction of radar echo trends. This study proposes a "Optical Flow" based extrapolation method for near-term forecasting to simulate and predict imminent weather situations. By analyzing the temporal variations of radar echoes, atmospheric motion features and vector information are extracted to provide physically meaningful precipitation forecasts. In forecast tests from 0 to 60 minutes, the optical flow method demonstrated excellent detection capabilities, with a Probability of Detection (POD) score exceeding 0.5 and a Critical Success Index (CSI) above 0.4 at the 30-minute forecast period, showing strong predictive performance. Furthermore, the method's computation time for the 30-minute forecast is approximately 5.4 seconds, meeting the real-time forecasting requirements. This study demonstrates that the optical flow method offers efficient computational performance and reliable forecasting ability in short-term precipitation prediction, providing an effective technical approach for this field. *(Abstract)*

Keywords: short-term precipitation forecasting, optical flow method, radar echo extrapolation, weather prediction, real-time forecasting

1 Introduction

Over the past few years, shifts in climate patterns have resulted in a rise of severe weather occurrences, such as heatwaves, droughts, and sudden torrential rainfall. As a type of extreme meteorological phenomenon, sudden torrential rainfall is marked by a swift build-up of significant moisture content, followed by a intense downfall of rain in a brief timeframe. Due to its abrupt nature, localized occurrence, and intense rainfall, such events have become a focal point of climate change research and pose significant challenges for forecasting and response. Sudden torrential rainfall can trigger secondary disasters[1],[2], such as mudslides, landslides, and urban flooding, which severely threaten social infrastructure, agriculture, and public safety.

W. Nie et al. (eds.), *Proceedings of the 2024 6th International Conference on Hydraulic, Civil and Construction Engineering (HCCE 2024)*, Atlantis Highlights in Engineering 37,
https://doi.org/10.2991/978-94-6463-726-7_44

Weather radar echo detection is a crucial tool for real-time weather monitoring, and nowcasting refers to the prediction of weather changes within a 0-2 hour timeframe[3]. The increasing frequency of sudden torrential rainfall events has heightened the demand for short-term precipitation forecasting. This paper explores thunderstorm identification, tracking, and detection techniques based on radar data, in pursuit of enhancing the precision and effectiveness of immediate weather predictions.

Currently, the optical motion flow method is widely used in radar echo trend prediction and is recognized for its unique advantages. This method estimates the movement speed and direction of precipitation areas by analyzing the changes in radar image sequences[4],[5]. Unlike machine learning approaches, the optical motion flow method is based on physical phenomena and directly extracts motion information from image variations, without the need for large amounts of labeled data.

The visual motion analysis approach enhances the accuracy and robustness of radar echo prediction[6], particularly when handling rapidly changing and highly localized echoes[7]. Additionally, the optical flow method does not rely on specific hardware configurations and can operate efficiently even with limited computational resources[8].

By analyzing the motion direction of radar echo signals, the visual motion analysis approach method can reliably determine the development course and direction of the signals.[9]. This study applies the optical flow method to nowcasting and develops radar echo forecasting products based on this approach[10]. For extrapolation forecasting, we employ a semi-Lagrangian scheme to project the echoes[11],[12],, which accounts for the nonlinear characteristics of atmospheric motion[13], helping to better preserve the rotational nature of the echoes and thereby improving forecast accuracy[14]. Through this method, we aim to provide more precise and reliable technical support for short-term precipitation nowcasting.

2 Method

2.1 Principles of Optical Flow Method

The visual motion analysis approach assumes that echo motion satisfies the Lagrangian conservation equation over a short time interval. Additionally, the method employs supplementary constraint equations to compute the optical motion flow field. Define $L(x, y, t)$ brightness level at coordinates (x, y) at the moment t. Following a period of Δt, the intensity value at the location transitions to $L(x + \Delta x,\ y + \Delta y,\ t + \Delta t)$. With the condition that $\Delta t \to 0$, the z value is considered approximately constant.

$$I(x,y,t) = L(x + u \cdot \Delta t,\ y + v \cdot \Delta y,\ t + \Delta t) \tag{1}$$

With u corresponds to the flow in the x-direction. With v represents the flow in the y-direction. Assuming a steady change in the brightness $L(x, y, t)$ over time Δt, equation (1) can be formulated using the Taylor series and omitting the second-order infinitesimal terms, leading to:

$$L(x,y,t) + \Delta x\frac{\partial L}{\partial x} + \Delta y\frac{\partial L}{\partial y} + \Delta t\frac{\partial L}{\partial t} = L(x,y,t) \tag{2}$$

In the equation, $\Delta x = u \cdot \Delta t$ and $\Delta y = v \cdot \Delta t$. Eliminating $L(x, y, t)$ from equation (2), after scaling both sides by Δt and evaluating the limit as $\Delta t \rightarrow 0$, we get:

$$\frac{\partial L}{\partial x}\frac{dx}{dt} + \frac{\partial L}{\partial y}\frac{dy}{dt} + \frac{\partial L}{\partial t} = 0 \tag{3}$$

Equation (3) is essentially the expanded form of $dL/dt=0$ and can be simplified as:

$$L_x u + L_y v + L_t = 0 \tag{4}$$

Equation (4) represents the optical flow constraint equation.

Let $\nabla L=(L_x, L_y)^T$, where ∇L denotes the gradient in space of the monochromatic image, with L_x being the time-based variation in grayscale intensity levels. The vector (u, v) mark the optical flow, with the optical flow field being an assembly of such vectors throughout the entire image. If the image is replaced by meteorological radar echo signals, with the detected targets being radar echoes rather than moving objects in the frame, then $L(x, y, t)$ serves as the reflectivity measure for the respective coordinate (x, y) at time t within the radar scan.

2.2 Lucas-Kanade algorithm for Optical motion Flow Method

The visual motion analysis approach method[15] is a classic computer vision technique for estimating motion from image sequences. The algorithm, developed by Bruce D. Lucas, along with Takeo Kanade in 1981, estimates the motion field for the entire scene by observing the trajectory of dominant attribute spots in an image sequence.

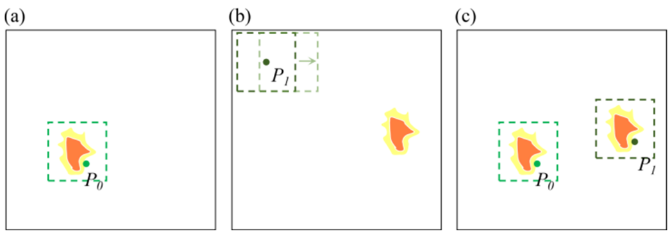

Fig. 1. Retrieval process of the L-Kanade optical flow method. (**a**) Cursor features in the first frame of the image; (**b**) Box frame used to search for the object's location in the second frame; (**c**) Calculation of the object's displacement based on the change in cursor position between consecutive frames.

As shown in Figure 1a, the Lucas-Kanade optical motion flow method begins by defining feature points P_0 in the first frame of the image. These feature points have distinctive visual characteristics, making them easy to track throughout the image sequence. For each feature point $P(x, y)$, a local box window centered at $P(x, y)$, denoted as B_1, is created, and the optical motion flow information within this box window is labeled as J_1. It is assumed that the optical flow within the local box window B_1 remains consistent with the movement of the feature point.

Next, as shown in Figure 1b, the method searches for the optical flow in the second capture of the photo using a box of the same size to find a region B_2 that has the highest similarity to J_1. The optical flow information in this region is labeled as J_2. By minimizing the difference between J_1 and J_2, we confirm $J_1 \approx J_2$, thus identifying B_2 as the position of B_1 in the second frame. Consequently, the location of the feature point in Figure 1a is determined in Figure 1b. As shown in Figure 1c, the object's displacement is calculated based on the changes in optical flow between the two frames.

Let E denote the error between J_1 and J_2. Within the local box window, the optical flow vector for each point is estimated by minimizing the error in the optical motion flow equation. The error in the optical motion flow estimation is given by:

$$E = \sum_{x \in \Omega} W^2(x)[\nabla I(x,t) \cdot \boldsymbol{V} + I_t(x,t)]^2 \tag{5}$$

In Equation (5), Ω represents the region centered at point P, $W^2(x)$ is the window function that denotes the weights of the points within the region, and $\boldsymbol{V}=(u, v)^T$ denotes the optical motion flow at point P.0

To ascertain the location of the box in Figure 1b associated with the smallest error E, the least squares approach is utilized to minimize the optical flow error. Based on the changes in the box positions between the preceding and subsequent frames, the displacement of the feature point P is computed.

Utilizing the Lucas and Kanade (LK) technique, radar echo movements are inferred through optical motion analysis. Although radar reflectivity can change over time, the interval between two radar scans is approximately 6 minutes, making these changes relatively minor. Therefore, it is reasonable to approximate that the radar images satisfy the optical motion flow constraint equation (4).

2.3 Semi-Lagrangian Extrapolation Method

To account for physical processes such as rotation and varying speeds during extrapolation, the semi-Lagrangian transport approach was utilized for the advancement of radar reflectivity images. The semi-Lagrangian method is known for its stability and accuracy and has been widely used in numerical forecasting models and climate models.

In the extrapolation of echoes, it is assumed that the physical quantities in space remain approximately constant during the temporal displacement. The following extrapolation formula is used[16]:

$$F'(t_0 + \Delta t, x) = F(t_0, x - s) \tag{6}$$

In Equation (6), F' represents the forecasted state of the radar echo field at $t_0+\Delta t$, F is the observed radar echo field at t_0, t_0 means the initial time, Δt means the look forward time, where s means the vector of displacement within the look forward time The formula assumes that the observed echo (Z) at position x - s at t_0 will move to position x at $t_0+\Delta t$ after a displacement of time Δt.

The Semi-Lagrangian extrapolation method apportions the prediction lookahead period Δt into N incremental stages for advancement, with each time step being Δt. In this study, a forward extrapolation method is used. The aggregate change in position throughout the forecast period equals the cumulative displacement across N increments, with the time step Δt set to 6 minutes.

The specific method for echo extrapolation employs the Reich-improved RPM-SL scheme[17].

2.4 Data Description

This examination incorporates radar data from the C-band dual-polarization system at Nanjing University, and also references data patterns from the studies led by Pan et al.[18], referred to as the NJU-CPOL dataset. The NJU-CPOL collection encompasses 268 rainfall occurrences spanning the years 2014 to 2019, comprising 35,133 individual data entries. The dataset has undergone quality control and Cartesian coordinate interpolation. All data used in this study have a horizontal grid spacing of 7 km, a grid size of 256 × 256, and a temporal resolution of 6 minutes.

3 Results

The NJU-CPOL data contains numerous cases of convective processes. This study selects representative convective events to test The efficacy of the optical motion flow technique in extrapolating radar composite reflectivity factors for forecasting intervals ranging from 0 to 60 minutes.

3.1 Case Study

The case selected involves a moving convective system, which is composed of a series of precipitation cloud clusters. Such systems typically move rapidly, causing short-duration, intense convective weather over a certain area, along with precipitation.

In this case, we identify representative feature points in the radar echo images by analyzing the image changes between successive time steps, and implementing the optical motion flow algorithm to gauge the movement of the significant component cues.

To obtain the displacement vector field of the entire flow field, we use the known valid feature point vectors as control points and apply an interpolation method to compute the global displacement vectors in the detection area. The interpolation algorithm used is the inverse distance weighting method, which assigns weights to the displacement vectors based on the distances between control points, thereby generating a smooth and continuous vector field in the unknown region.

As shown in Figure 2, panel 2a illustrates the vector displacement trends of the feature points computed using the optical flow method, while panel 2b shows the spatial distribution of vector displacements obtained by interpolating the vector displacement trends across the entire observation area.

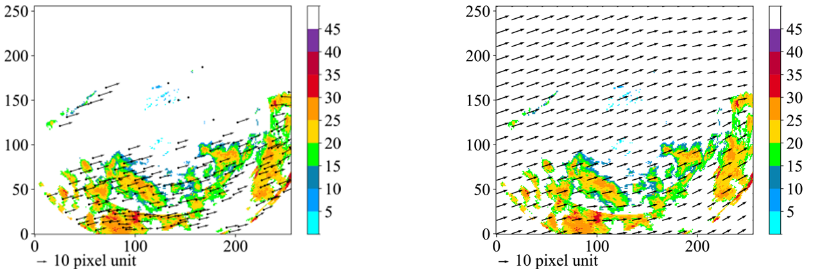

(a) (b)

Fig. 2. Displacement vector field obtained using the optical motion flow method. **(a)** Displacement vectors of feature points; **(b)** Interpolated displacement vector field for the entire detection area.

To predict the radar signal echo trends, a semi-Lagrangian advection extrapolation scheme is applied. This method calculates the displacement of the physical quantities in the grid field based on the wind speed.

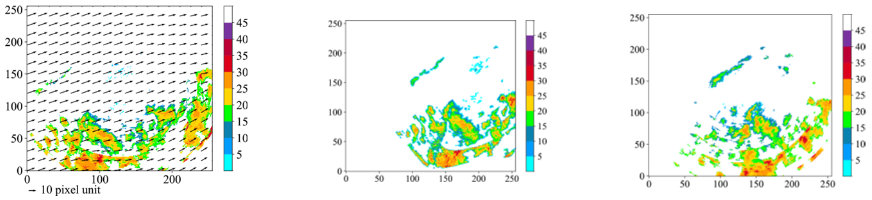

(a) (b) (c)

Fig. 3. Comparing the derived echo predictions with themeasured data. **(a)** Echo features at time t = 0; **(b)** Extrapolated echo features 30 minutes after t = 0; (c) Actual echo features at t = 30 minutes.

As shown in Figure 3, panel 3a presents the echo state and spatial vector field at initial time. Based on this original state (t = 0), the prediction model is used to simulate the evolution of the echo over the next 30 minutes, with the results shown in panel 3b. Panel 3c displays the actual radar echo distribution at t = 30 minutes. Comparing the predicted result in panel 3b with the actual observation in panel 3c, it can be observed that both have a high similarity in the shape and distribution of the echoes, despite some differences. These discrepancies are mainly attributed to the dynamic characteristics of the thunderstorm system. Specifically, as the thunderstorm moves, its internal convective activity continuously evolves, which may lead to deviations between the actual echo development and the predicted results.

As shown in Figure 4, panel 4a presents the predicted echo features extrapolated 60 minutes ahead, based on the current radar echo state. The predicted result generally matches the actual observed distribution shown in panel 4b in terms of overall shape, but there are some notable differences in detail. These differences are primarily caused by external signals at the boundaries of the detection area. Overall, the echo extrapolation method demonstrates practical effectiveness.

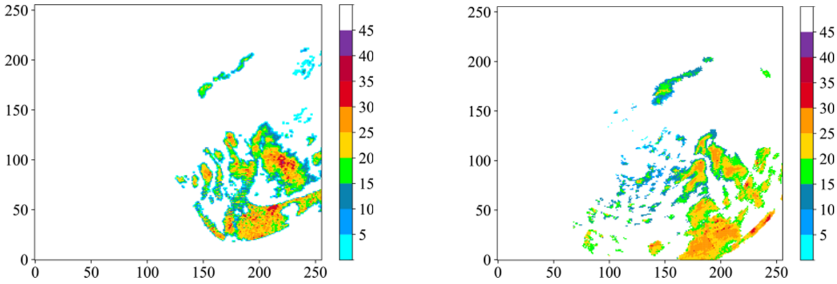

(a) (b)

Fig. 4. Comparison of the extrapolated echo results with the measured data. **(a)** Extrapolated echo features 60 minutes after t = 0; **(b)** Actual echo features at t = 60 minutes.

Furthermore, further observations in this case reveal that during the 30-minute extrapolation period, the echoes near the boundary are relatively unaffected by the boundary conditions. However, as the extrapolation period extends to 60 minutes, the influence of the boundary conditions becomes significantly more pronounced. This may be related to the speed and complexity of the evolution of the weather system.

3.2 Forecast Verification

To fully assess the reliability of the optical flow and cross-correlation techniques for the forecasting of radar echo behavior, we employed a grid-point-based statistical comparison approach. Specifically, we first analyzed the distribution of forecasted echoes and the corresponding observed echoes at the same grid points. Each grid point was then assessed based on the following criteria:

a. Hit: If an observed echo is present at a grid point and a forecasted echo is also present at that point, it is considered a hit.

b. Miss: If an observed echo is present at a grid point but no forecasted echo is present, it is considered a miss.

c. False Alarm: If no observed echo is present at a grid point but a forecasted echo is present, it is considered a false alarm.

We computed the Probability of Detection (POD). This calculation relied on a specific set of formulas:

$$POD = \frac{TP}{TP+FN} \tag{7}$$

We determined the Critical Success Index (CSI). This calculation relied on a specific set of formulas:

$$Csi = \frac{TP}{TP+FP+FN} \tag{8}$$

In this context, TP (means: True Positive) refers to the count of accurately identified targets, FN (means: False Negative) indicates the number of targets that were overlooked, and FP (means: False Positive) signifies the count of incorrect alerts.

Subsequently, the simulations from the previous case are assessed using the Hit Rate (POD) and the Critical Success Factors Index (CSI) as evaluation metrics.

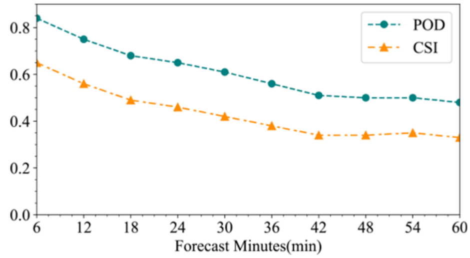

Fig. 5. Results of the POD and CSI scores.

Figure 5 displays the results of echo extrapolation. These results are based on two key metrics. The initial performance indicator is termed the Probability of Detection, or POD. Another key performance measure is the Critical Success Factors Index, abbreviated as CSI. The POD scores are generally higher than the CSI scores, as the CSI metric takes into account the "false alarm" conditions.

As the forecast lead time increases, we observe a decline in both POD and CSI scores across all cases. Specifically, as the forecast lead time progresses from t=0 to t=60 minutes, the average POD score decreases from approximately 0.9 to around 0.5, and the CSI score also declines correspondingly. This trend suggests that as the forecast lead time extends, systematic errors increase, leading to a decrease in forecast reliability. This may be attributed to the current limitations of extrapolation models in accurately simulating the physical mechanisms of thunderstorm initiation, development, and dissipation.

3.3 Efficiency of the Computational Model

To evaluate the model's computational speed, we timed its processing on a Xeon E5-2650 server. The model, coded in Python with NumPy, logged both its extrapolation duration and computational usage.

Table 1. Extrapolation time and computational consumption

Extrapolation time	Computational Cost
6 min	1.9 s
18 min	3.5 s
30 min	5.4 s
42 min	6.8 s
60 min	9.5 s

As shown in Table 1, for echo extrapolation, the computational time increases with the extension of the extrapolation period, though this increase is not linear. Since the model is coded in Python, further enhancements in computational efficiency are possible.

4 Conclusions

This study employs the optical motion flow algorithm. It combines this with semi-Lagrangian backward extrapolation. The purpose is to forecast radar echoes up to 60 minutes into the future. The forecasts are then compared to observational data. The following conclusions were made based on the analysis.

(1) The LK algorithm for optical flow demonstrates good performance in extrapolating radar echoes associated with nonlinear motion. In the case study, the thunderstorm system exhibited a clear turning motion during its movement, and the LK algorithm for optical flow successfully captured this motion characteristic, confirming the method's effectiveness in handling nonlinear motion.

(2) When combined with the semi-Lagrangian extrapolation method, the LK algorithm for optical flow effectively preserves the characteristic shape of the thunderstorm system. Extrapolation tests demonstrate that the method maintains the shape of the convective cloud system as it moves.

(3) The LK algorithm for optical flow has certain limitations. As the forecast time increases, echo signals from the boundaries of the detection area are introduced, and the LK algorithm for optical flow cannot account for boundary conditions. These limitations lead to a gradual degradation in forecast accuracy.

The Lucas-Kanade algorithm’s utility in optical motion flow for thunderstorm tracking is notable, yet its forecasting of convective activity specifics requires enhancement. Future research directions include refining the model to better simulate physical processes and considering the addition of deep learning to sharpen echo prediction during both formation and dissipation stages.

References

1. Guo Jun, et al. 2023. Study on optimization and combination strategy of multiple daily runoff prediction models coupled with physical mechanism and LSTM. J. Hydrol. 624, 129969.
2. Guo Jun, et al. 2020. Vulnerability Assessment for Power Transmission Lines under Typhoon Weather Based on a Cascading Failure State Transition Diagram[J]. Energies, 13: 3681.
3. Alfieri, L ; P. Claps ; F. Laio . Time-dependent Z-R relationships for estimating rainfall fields from radar measurements. Natural Hazards & Earth System Sciences 10.1(2010):149-158.
4. Shukla Bipasha Paul, et al. Satellite based rainfall nowcasting using geospatial techniques[J].METEOROLOGY AND ATMOSPHERIC PHYSICS, 2025,137(1):1-16.
5. Wei Xiangqian, et al. 2024. "Numerical Simulation of Terrain-Adaptive Wind Field Model Under Complex Terrain Conditions" Water 16, no. 15: 2138.

6. Lima Jonathan A. S., et al. SynFlowMap: A synchronized optical flow remapping for video motion magnification[J].SIGNAL PROCESSING-IMAGE COMMUNICATION, 2025, 130.
7. Shan Liang, et al. A lightweight optical flow model for particle image velocimetry[J].FLOW MEASUREMENT AND INSTRUMENTATION, 2025, 102.
8. Cakir Bora O. O., Lavagnoli Sergio. Assessment and application of optical flow in background-oriented schlieren for compressible flows[J].EXPERIMENTS IN FLUIDS, 2023, 64(1):1-20.
9. Wang Jiahui. The application of improved SURF optical flow algorithm in seismic support safety monitoring system[J].International Journal of Cognitive Computing in Engineering, 2025, 6(1):109-119.
10. Zhang, Chengwei; Zhou,Xudong; Zhuge, Xiaoyong;Xu, Meng. Learnable Optical Flow Network for Radar Echo Extrapolation.IEEE JOURNAL OF SELECTED TOPICS IN APPLIED EARTH OBSERVATIONS AND REMOTE SENSING, 2021.14, 1260-1266.
11. Peng Dunlu, et al. Enhanced optic-flow extrapolation for Doppler radar nowcasting with Dynamic Weight Attention[J].EXPERT SYSTEMS WITH APPLICATIONS, 2025, 267.
12. Wei Xiangqian, et al. 2024. "Applicability Study of Euler–Lagrange Integration Scheme in Constructing Small-Scale Atmospheric Dynamics Models" Atmosphere 15, no. 6: 644.
13. Jones William K. K.;Christensen Matthew W. W.; Stier Philip. A semi-Lagrangian method for detecting and tracking deep convective clouds in geostationary satellite observations.ATMOSPHERIC MEASUREMENT TECHNIQUES, 2023.16(4), 1043-1059.
14. Jiakai, ZHU; Jianhua, DAI. A rain-type adaptive optical flow method and its application in tropical cyclone rainfall nowcasting.Frontiers of Earth Science, 2022.16(2), 248-264.
15. He Yu, Yap Kim-Hui. A nonlinear least square technique for simultaneous image registration and super-resolution[J].IEEE TRANSACTIONS ON IMAGE PROCESSING, 2007, 16(11):2830-2841.
16. Clancy Colm, et al. A class of semi-implicit predictor-corrector schemes for the time integration of atmospheric models[J].JOURNAL OF COMPUTATIONAL PHYSICS, 2013, 250(1):665-684.
17. Reich, Sebastian . "An explicit and conservative remapping strategy for semi-Lagrangian advection." Atmospheric Science Letters 8.2(2007):58-63.
18. Fox Neil I, et al. Applications of Bayesian Procrustes shape analysis to ensemble radar reflectivity nowcast verification[J].ATMOSPHERIC RESEARCH, 2016, 176:75-86.